

This is the final peer-reviewed accepted manuscript of:

**S. Mignardi, M. J. Arpaio, C. Buratti, E. M. Vitucci, F. Fuschini and R. Verdone,
"Performance Evaluation of UAV-Aided Mobile Networks by Means of Ray
Launching Generated REMs"**

in *2020 30th International Telecommunication Networks and Applications
Conference (ITNAC)*, Melbourne, VIC, Australia, 2020

The final published version is available online at:

<https://doi.org/10.1109/ITNAC50341.2020.9315177>

Rights / License:

The terms and conditions for the reuse of this version of the manuscript are specified in the publishing policy. For all terms of use and more information see the publisher's website.

This item was downloaded from IRIS Università di Bologna (<https://cris.unibo.it/>)

When citing, please refer to the published version.

Performance Evaluation of UAV-Aided Mobile Networks by Means of Ray Launching Generated REMs

Silvia Mignardi, Maximilian J. Arpaio, Chiara Buratti, Enrico M. Vitucci, Franco Fuschini, Roberto Verdone
DEI - Department of Electrical, Electronic and Information Engineering "G. Marconi"
Alma Mater Studiorum University of Bologna
Bologna, Italy

{silvia.mignardi, maximilian.arpaio, c.buratti, enricomaria.vitucci, franco.fuschini, roberto.verdone}@unibo.it

Abstract— Unmanned Aerial Vehicles (UAV), also known as drones, are receiving increasing attention as enablers for many emerging technologies and applications, a trend likely to continue in the next future. In this regard, using Unmanned Aerial Base Stations (UABSs), i.e. base stations carried by UAVs, is one of the most promising means to offer coverage and capacity in 5G applications to those users that are not being served by terrestrial base stations. In this paper, we propose a novel approach for trajectory design and Radio Resource Management (RRM) in UAV-aided networks using information retrieved from precise Radio Environmental Map (REM) based on Ray Launching (RL) simulations for RF propagation and narrow band estimations. Furthermore, we consider different possible models for antennas to be installed on multiple UABSs as well as proper RRM strategies which are able to take advantage of REM inputs. Simulation results will show the performance achieved by the system for the different approaches and it will compare them with the previous use of statistical models.

Keywords— *Graphics Processing Unit GPU, Radio Resource Management, Ray Launching, Trajectory Optimisation, Unmanned Aerial Vehicles.*

I. INTRODUCTION

The fifth generation (5G) of mobile radio networks will be employed in many application domains like the Internet of Things (IoT) and connected vehicles, which will dramatically increase the number of devices [1]. Intuitively, a higher density of connected devices will produce a larger standard deviation in the traffic generation process: a network deployment based on average or peak traffic predictions will produce highly suboptimal results. Therefore, future networks will need to be much more flexible than in the past and should be able to react smoothly and automatically to the fast time-space variations of any traffic demand. This can be achieved by moving the network infrastructure and tailor it according to actual traffic needs. Thanks to the ability to fly almost freely anywhere and whenever the highest needs arise, aerial platforms like Unmanned Aerial Vehicles (UAVs), become excellent candidates as nodes of any future network.

Recent studies on UAVs show that their use as Unmanned Aerial Base Stations (UABSs) [2] might be an efficient complement to traditional Terrestrial Base Stations (TBSs) [3]

or might even substitute TBSs in emergencies [4]. The advantages in using UAVs are manifold: i) UAVs can fly where TBSs cannot offer good coverage and capacity; ii) UAVs can satisfy traffic demand when needed, with a proper planned trajectory; iii) UAVs can stand out against the urban layout more than terrestrial BSs, thus benefitting from better overall propagation conditions for both the access link toward the ground users and the backhaul. For these reasons, in the previous years, the interest in UABSs has gradually increased and many works have been published. The first results about the use of UAV-aided networks were related to link-level considerations, where the main focus was on the characterization of the Path Loss (PL). For instance, in [5] the effect of the user-UAV angle vs. ground plane is studied as a function of the drone height; it was shown that these parameters have a non-negligible impact on the mean PL and the shadowing formulation. In very recent activities of 3GPP standardization body, UAVs take a relevant role in being part of 5G or beyond 5G - future - wireless networks. The new release includes important documents which further study communication with UAVs [6, 7] (started with considering UAVs as User Equipment (UE) in [8]), where UxNB becomes the acronym for UAVs with on-board radio access (functioning either as eNB relay or as an eNB itself). This is a considerable result for such an emerging technology. Among many works on UABSs, [9] finds an acceptable trade-off between coverage, capacity, and connectivity, and [10] minimises the number of flying BSs needed to provide coverage to a group of users. However, many works related to UABSs assume free-space path loss propagation environment. This is a quite simplistic assumption since the channel model may vary significantly depending on the task location and especially in urban environments. Existing Air-To-Ground (A2G) models try to capture the variations of the channel from typical UABSs heights, but are rarely tested and compared in practical scenarios. In this regard, is important to mention [11] since it proposes a method to reconstruct a radio map of the considered environment with UAVs. Through the proposed approach, it is possible to let a UAV fly offline to reconstruct and store in its memory the radio map. Authors in a previous work [12] first propose a possible approach to employ Radio Environmental Maps (REMs) in UAV-networks planning, but only with a simple and parametric emulation of radio maps.

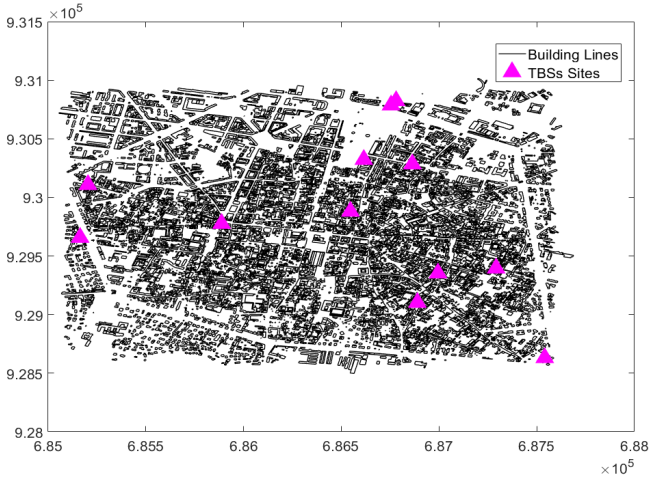


Fig. 1. Bologna city centre, urban environmental 3D model

To further enrich the above cited works, we investigate the performance of a heterogeneous network composed of both TBSs and UABSs by developing a database of coverage maps of an urban environment using a self-developed Ray Launching (RL) software.

Our goal is to convert such database into inputs for the network controller with the aim to manage radio resources and plan UABSs trajectories.

We can summarize our contribution as follows:

- We generate *coverage maps* using a properly designed RL simulator, with many different UAV settings;
- We propose a model for an emerging technology, that considers the generated coverage maps as an input to both design UABS trajectories and to apply radio resource management techniques;
- We compare the performance of the proposed model against literature-based models of the A2G channel, with the aim to discuss the feasibility of the RL database based on the simulated received power *a priori* for different UAV positions.

The paper is organised as follows. After a brief introduction in the current Section I, Section II describes the scenario and the network elements involved. The channel model and RL environment are also introduced. Section III presents the system model and algorithms. Finally, numerical results and conclusions are reported in Sections IV and V, respectively.

II. REFERENCE SCENARIO

To include proper RL estimations in our model, we need to consider a real map of an urban city as the service area. In our case, we selected the city centre map of Bologna, Italy. It is used in UTM coordinates as reference system over an area of around 6.5 Km² (see Fig. 1). The TBSs locations are emulated starting from the actual network service deployment of a city operator for UMTS/LTE, with a total of N_{TBS} legacy BSs. The UABSs are initially parked in one of the TBSs, that becomes the starting point of their flight.

TABLE I. SCENARIO AND NETWORK PARAMETERS

Parameter Definition	Value
N_{TBS}	36
v	20 m/s
B	200 MB
S_{min}	100 Mb/s
T_w	15 s
f_c	3.5 GHz
TBS bandwidth	100 MHz
Subcarrier spacing	30 kHz
Number of subcarriers in each PRB	12
Minimum SNR value for connection	10 dB
Transmit power of TBSs	36 dBm
Antenna gain of TBSs	12 dB
Transmit power of UABSs	10 dBm

Both BS types operate as a 5G network system with carrier frequency $f_c=3.5$ GHz, where Radio Resources (RRs) are organised in Physical Resource Blocks (PRBs) and frames of 20 s. The maximum capacity per frame is 7.2 Mbps.

A. Traffic Model and User Distribution

To comply with RL simulations, users are randomly distributed in the outdoor space of the city centre with a mean density λ . We assume users in the area are asking for a video download of size B , that has a minimum throughput requirement denoted as S_{min} . Moreover, each user is willing to wait a maximum time T_w , otherwise it leaves the network. As commonly seen in the literature, we assume the UABSs can estimate users' locations through network information. The values of the scenario parameters are presented in Table I. The RL and network simulations map is also shown in Fig. 1, together with the TBSs placement.

B. Statistical Channel Model and Data rate

In this paper, we compare the use of RL and REM as an emerging technology with common channel models. The communication channels investigated are both the TBS-user and UABS-user links, the latter being the A2G model. We consider the received power, P_{rx} , is computed as a function of the transmitted power P_{tx} , as $P_{rx}[\text{dBm}] = P_{tx}[\text{dBm}] + G_{tx}[\text{dB}] - L[\text{dB}]$. Then, to investigate the propagation comparison, we compute the channel loss $L[\text{dB}]$ through RL as described in Sec. II.C. For what concerns the user links with TBSs, the channel model employed is the one used in [12], with a propagation coefficient of 3.6 and a shadowing variance of 6 dB. For the A2G link, the propagation model is based on the one described in [5] for an urban environment. According to this model, connections between drone and ground users can either be LoS or Non-Line-Of-Sight (NLoS). When the connections occur in NLoS, the signals travel in LoS before

interacting with objects located close to the ground, which results in shadowing effect.

We denote as pLoS the probability that the UAV and users are in LoS. The probability pLoS depends on the given elevation angle θ and it is computed according to the following equation

$$p_{LoS} = \frac{1}{1 + \alpha \exp\left(-\beta \left[\frac{180}{\pi} \theta - \alpha\right]\right)} \quad (1)$$

with α and β being environment-dependent constants, i.e., rural, urban, dense urban, etc. and adopted as given in [5].

The PL model is given as:

$$L_\eta [dB] = 20 \log\left(\frac{4\pi f_c d}{c}\right) + \xi_\eta \quad (2)$$

where ξ is the shadowing coefficient which is set as described in [5], and $\eta = \{\text{LoS, NLoS}\}$ represents the link condition either being LoS or of NLoS. In particular, the value of η depends on pLoS in Eq. (1) for each link (one realization is computed for each user in every UABS location), and strongly impacts the value of ξ . Then, c is the speed of light, f_c is the central frequency, and d is the transmitter-receiver distance.

Then, data rate R is evaluated by means of the Shannon capacity, independently from the $L[dB]$ estimation:

$$R = B_c \log_2\left(\frac{P_n}{P_n} + 1\right) \quad (3)$$

where B_c is the signal bandwidth in [Hz] and P_n is the noise power [W]. One further assumption is made in A2G channels, that is UABSs can estimate the loss of a link before reaching it. This is not needed in the case REM are available, because it refers to a database that is known *a priori*.

C. Deterministic Channel model through Ray Launching Simulations based on NVIDIA GPU Acceleration

The Discrete Environment-Driven RL model (DEDRL), has been introduced for the first time in [13]. The software relies on a digitalised urban model of the city where each building is a polygon with a defined shape, material, position, and height; this is the same map as it can be seen in in Fig. 1. The model is discrete, i.e. the building walls are properly discretized into tiles with a predetermined size. In addition to seamless space tessellation, other advanced features have been implemented to achieve very high accuracy while drastically reducing computation time. The main advantage of discretization is that the tile centres can be assumed as fixed points, therefore all the visibility relations among the tiles can be pre-computed and properly stored into a visibility matrix.

This visibility pre-processing is carried out only once, for a single simulation scenario.

TABLE II. PARAMETERS FOR RL SIMULATIONS

Parameter Definition	Value
Frequency	3.5 GHz
Altitude	{50, 75, 100} m AGL
Drone Position	distributed square grid of 1156 points
Number of interactions	5 bounces, 5 reflections, 2 diffractions, 1 scatter
Number of combined interactions	3 among reflections and diffractions(max) 3 among diffractions and scatter(max)
Scattering coefficient	0.4
Relative permittivity	5
Wall conductivity	0.01 S/m

Of paramount relevance is the fact that both the visibility pre-processing and the bouncing of the ray tubes in RL, are suitable to be parallelized into Graphics Processing Units (GPUs) and can be thus run using NVIDIA cards. Typical computation times for complete predictions range from a few seconds to tens of minutes, depending on the size of the urban scenario and the characteristics of the transmitting site.

Based on the outcomes in [12] and [14], this paper employs realistic REMs as an emerging application to enhance trajectory optimisation, properly built via a complete set of fast RL simulations immediately available to the designer. Simulations were run on a commercial workstation, equipped with an Intel(R) Xeon(R) CPU E5-2620 v4 @ 2.10 GHz [8c/16t] and 48 Gb RAM. Simulations were boosted by means of a Titan Xp card manufactured by NVIDIA, configured for GPU computing acceleration. The simulation parameters, set accordingly with the network simulator, are shown in Table II.

III. SYSTEM MODEL

In the service area, users may be served by either the TBSs or UABSs. This is possible because we assume seamless communication between the network orchestrator and each BS in the control plane. The selection of the best server and Radio Resource Management (RRM) is made following principles of fairness and network throughput increase. For example, the orchestrator chooses the best server for a user depending on the strongest link in terms of PL or selects the nearest UABS if neighbouring TBSs are overloaded by the high traffic demand. Then, the RRM is made with a Round Robin algorithm, followed by Proportional Fair if spare radio resources are present.

A. UABS Trajectory Design

The dynamic trajectory design follows the algorithm proposed in [16]. Therefore, the overall system performs the following steps:

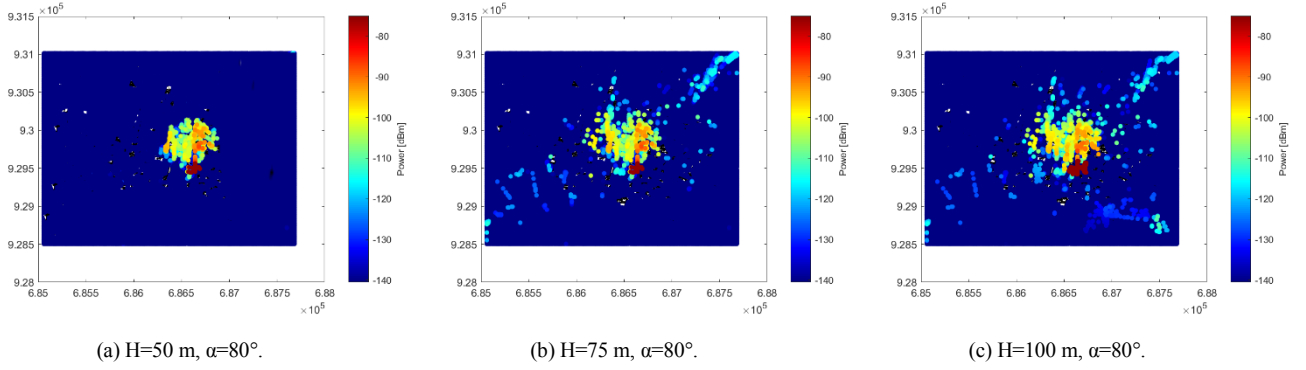


Fig.2 Coverage map over Bologna city centre, examples of received power at different heights for 3.5GHz

- the network orchestrator groups the users remained not reachable (e.g. low SNR or resource overload) from the TBSs in K clusters [15];
- for each cluster ($i = 1, \dots, K$), its centroid is calculated.
- for each centroid ($i = 1, \dots, K$), a cost function C_i is computed.
- the centroid having the smallest cost is selected and we denote its distance from the UABS as d_c .
- the UABS flies towards the chosen centroid along a segment lasting a time interval d_c/v , where v is the UAV speed.
- during its flight from one centroid to another, the UABS serves all users along its way [15].

When the UABS reaches a centroid, this procedure is repeated.

The cost function C_i is computed as:

$$C_i = \frac{d_i}{d_{th}} \cdot \frac{\delta_i}{\delta_{max}} \cdot \frac{W_i}{W_{max}} \cdot \frac{S_{min}^{(cl)}}{S_i^{(cl)}} \cdot (1+B) \quad (4)$$

where d_i and δ_i represent the distance of the i -th centroid to the drone and the user density, respectively. d_{th} and δ_{max} are normalizing factors with the maximum value of distances and densities, respectively. Further, the fraction $\frac{W_i}{W_{max}}$ accounts for the resource reuse, where W_i are the RRs already used by the TBSs under the UAV coverage area and W_{max} normalises the factor with the maximum available.

The fraction $\frac{S_{min}^{(cl)}}{S_i^{(cl)}}$ considers the estimated Sum

Throughput (ST) obtained in the i -th centroid $S_i^{(cl)}$. $S_{min}^{(cl)}$ is the minimum throughput achievable in the current set of identified clusters. The term $(1+B)$ provides spatial fairness.

It is important to note that the ST is obtained by computing the link budget and PL of every user to its BS. Therefore, when a statistical model is employed to compute the A2G PL, the ST is an estimation from the given formulation (Sec. II.B). Conversely, when the RL database is employed, the PL sample corresponding to the user position is considered for the actual loss. For this reason, we can effectively state that our trajectory planning is based on a REM knowledge. Please note, the PL sample – stored in a database - is always updated in time with regards to the UABS and users' positions. Therefore, the REM accuracy is based on the discretization of the UABS possible positions in the map of the service area and the variations of fast fading.

B. UABS Antenna System

We consider UABSs equipped with a directional antenna pointing perpendicular towards the ground, with a fixed aperture angle α . This angle α is simply the ideal and symmetrical radiation cone of the antenna within which, to keep the RL simulations affordable, we assumed an ideal antenna with constant gain inside its radiation cone - which depends on the angle α - and consequently negligible side lobes. The area covered by the UABSs (i.e footprint) on the ground will not assume a circular shape depending on the aperture angle, because a user is under actual coverage depending on its estimated PL. However, the PL, and consequently the UABS footprint, tend to depend on the UABS height [15]: the footprint area increases as the UABS altitude becomes higher, as it can be seen in Fig.2 a) to c). We then assume that the UABS antenna gain depends on α as $G_\alpha = 29000/(\alpha)^2$. We add to this value, a 3 dB gain in order to account for a minimum level of gain even when α is very large.

Therefore, we can state that the larger the UAV height, the larger the footprint. Consequently, the number of users that can be served by the UABSs (i.e., are under its coverage area) might increase. On the other hand, by fixing h , the larger is the angle α , the larger is the footprint and the smaller is the antenna gain.

IV. SIMULATION RESULTS AND DISCUSSION

The network performance is obtained from a network simulator developed for this purpose.

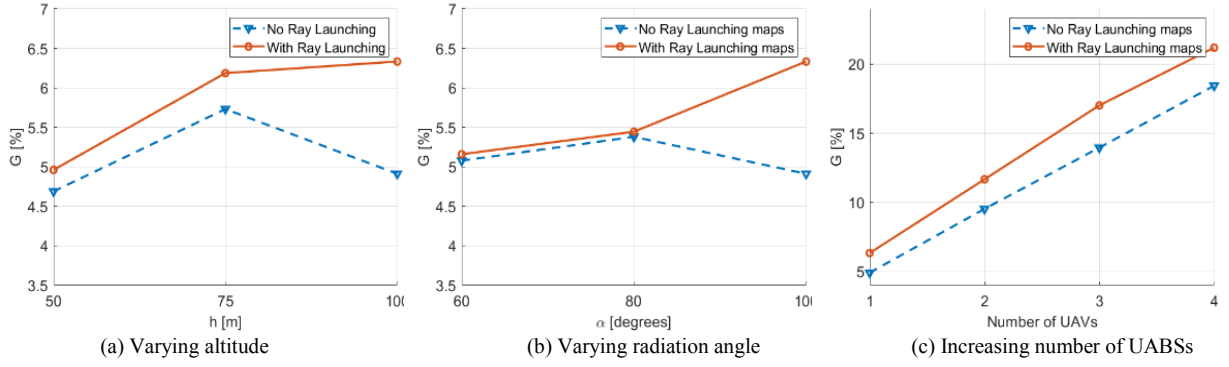


Fig.3. Throughput gain of a flying UABS while varying UABS parameters

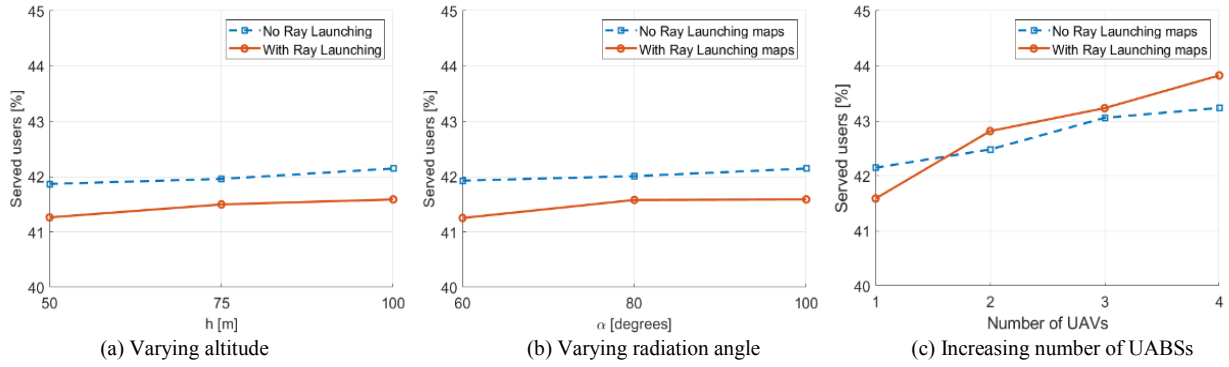


Fig. 4. Percentage of served users while varying UABS parameters

Both RL and network simulations run on a MATLAB environment to ease the joint computation and keep outcome files in the same format.

The metric chosen for the analysis of the results is the network throughput gain G , computed following Eq. (5):

$$G = \frac{S_{UABS}}{S_{tot}} \quad (5)$$

The terms S_{UABS} and S_{tot} represent the sum of the users' throughput obtained by the UAV only and by the entire network respectively, that is when both TBSs and UABSs are considered. This, together with the percentage of served users in the service area, lead to represent the network Key Performance Indicators. Subsequently, performance is computed to study the difference between channel estimation through known models and retrieving a previously calculated value of PL over a REM database. This database is made of a set of REMs calculated on each of the 1156 drone positions, as stated before in Table II, which ensure the reliability of the constructed REMs, minimising the need for any spatial interpolation [17].

This leads to an average distance of around 70 m between each consecutive drone position, enhancing the accuracy of the database on one hand, but increasing the complexity on the other hand. Note that PL evaluations influence not only the

channel gain for each user but also the UABSs' trajectory design through sum throughput estimation. The cluster cardinality K is not given as a fixed value but computed depending on the network load. In fact, it holds $K=N_{uu}/N_{uc}$, where N_{uu} is the number of unsatisfied users and N_{uc} represents the average number of users per cluster for each time unit. Fig.3 and Fig.4 in the next page simulate a traffic load where an average number of more than 3000 users are asking for service. They compare the performance by varying different parameters of the UABSs:

- UABS altitude, between 50 m and 100 m, where the propagation environment is more critical, especially in an urban scenario
- antenna radiation angle (and consequently the transmission gain), increasing from 60 to 100 degrees.
- the number of UABSs providing service to users in the urban area.

These pictures include two curves representing the simulation results for the different channel models. Fig. 3 shows the network performance in terms of throughput gain, while Fig. 4 in terms of the percentage of served users within the service area, when both TBSs and drones are available.

In general, Fig. 3 is the set of plots proving a higher difference in performance between the two computations for channel propagation. In particular, we have up to 1.5%

throughput gain improvement in network performance while varying both aperture angle and UABS height. Moreover, in the case of multiple UABSs, the gap between the two model results increases the gain of up to 5%. This is reasonable because the increased number of links in the network, due to more aerial stations, sharpens the difference.

In all simulation runs, the statistical model provides the worst-case scenario, but the trend of the two curves is similar except for small (with respect to the absolute value) statistical variations. This result shows that, as we expected from a correct RL development and a fair statistical ATG channel, the two applied propagation models work in a comparable manner. Having the same network trend also proves the implementation accuracy, as a similar network behaviour was anticipated.

One may also note the maximum created by simulation with statistical models in Figs 3a) and 3b). While a maximum for the altitude was expected because of the trade-off between distance and LoS probability, one for the aperture angle was not. In this case, statistical models indicate an optimal trade-off in choosing both the altitude and the radiation angle, that the RL model shows it is not applicable for the scenario of Bologna city centre. This trade-off should be instead with different values, and the results from statistical models may be misleading and altering the network planning made by a mobile operator. However, please note that the metric analysed here is in terms of overall network throughput, which is not a fairness metric among different users, but helps in understanding the efficacy of the system model versus applied costs.

V. CONCLUSION

In this paper, we studied the performance of a network made of both TBSs and UABSs having the knowledge of the REM in an urban environment. A RL simulator has been employed to enhance the construction of the REM for the network in a fast and prompt way. We proposed a model obtained from a network having a priori knowledge of the REM in its service area to both outline UABSs trajectories and make efficient RRM; then we compared the achieved results with a model from the literature of the A2G channel.

Results show the presence of a difference between simulations with RL and statistical models, as expected. The gap can demonstrate the significance of having RL accuracy in a realistic scenario, where the use of resources changes based on how strong is the A2G link. In this way, we can demonstrate in a realistic scenario the significance of having RL accuracy in terms of propagation evaluation, since the use of radio resources may vary depending on how strong is the A2G link. Still, if there is no database storage availability, the network performance given by statistical models might be satisfactory.

Further works will focus on additional and different environments - with a more dense scenario or higher buildings - and dynamic adaptation of the antenna radiation angle α with the aim to optimize the served users according to their density and the specific position of the UAVs.

ACKNOWLEDGEMENT

This work has been partly developed in the framework of the COST Action CA15104 "IRACON". Besides, the authors wish to express their gratitude to NVIDIA Corporation with the donation of the Titan Xp GPU card used for this research.

REFERENCES

- [1] CISCO, C.V. Forecast, "Cisco visual networking index: Global mobile data traffic forecast update 2016-2021", (2017).
- [2] Y. Zeng, R. Zhang, T. J. Lim, "Wireless Communications with Unmanned Aerial Vehicles: Opportunities and Challenges", *IEEE Communication Magazine* 54 (5).
- [3] F. Mohammed, et al., "UAVs for smart cities: Opportunities and challenges", 2014 International Conference on Unmanned Aircraft Systems (ICUAS), 2014, pp. 267-273.
- [4] R. M. Santos, et al., "Flying real-time network for disaster assistance", International Conference on Ubiquitous Computing and Ambient Intelligence, 2017.
- [5] A. Al-Hourani, S. Kandeepan, S. Lardner, "Optimal lap altitude for maximum coverage", *IEEE Wireless Communications Letters* 3 (6) (2014) 569-572.
- [6] 3GPP TS 22.289 V17.1.0, "Enhancement for Un-manned Aerial Vehicles," Sep 2019. [Online]. Available: <http://www.3gpp.org/ftp/Specs/archive/22series/22.125/22125-10.zip>
- [7] 3GPP TS 22.125 V17.1.0, "Unmanned Aerial System (UAS) support in 3GPP," Dec 2019. [Online]. Available: <http://www.3gpp.org/ftp/Specs/archive/22series/22.125/22125-10.zip>
- [8] 3GPP TS 36.777, "Enhanced LTE support for aerial vehicles," 2017. [Online]. Available: <ftp://www.3gpp.org/specs/archive/36series/36.777>
- [9] E. Yanmaz, "Connectivity versus area coverage in unmanned aerial vehicle networks", 2012 IEEE International Conference on Communications (ICC), 2012, pp. 719-723.
- [10] J. Lyu, Y. Zeng, R. Zhang, T. J. Lim, "Placement optimization of uav-mounted mobile base stations", *IEEE Comm. Letters*.
- [11] J. Chen, U. Yatnalli, D. Gesbert, "Learning radio maps for UAV-aided wireless networks: A segmented regression approach", 2017 IEEE International Conference on Communications (ICC).
- [12] S. Mignardi, C. Buratti, R. Verdone, "On the impact of radio channel over rem-aware UAV-aided mobile networks", 22nd International ITG Workshop on Smart Antennas, 2018, pp. 1-6.
- [13] J. S. Lu, E. M. Vitucci, V. Degli-Esposti, F. Fuschini, M. Barbiroli, J. A. Blaha, H. L. Bertoni, "A discrete environment driven GPU-based ray launching algorithm", *IEEE Transactions on Antennas and Propagation* 67 (2) (2019) 1180-1192.
- [14] M. J. Arpaio, E.M. Vitucci, M. Barbiroli, V. Degli-Esposti, D. Masotti, F. Fuschini, "Narrowband Characteristics of Air-to-Ground Propagation for UAV Assisted Networks in Urban Environments By Means of Fast Ray-Launching Simulations", 2020 IEEE 91st Vehicular Technology Conference (VTC2020-Spring), Antwerp, Belgium, 25-28 May 2020.
- [15] M. Deruyck, A. Marri, S. Mignardi, L. Martens, W. Joseph, R. Verdone, "Performance evaluation of the dynamic trajectory design for an unmanned aerial base station in a single frequency network", 2017 IEEE Personal, Indoor, and Mobile Radio Communications (PIMRC).
- [16] S. Mignardi, R. Verdone, "Joint path and radio resource management for UAVs supporting mobile radio networks", 2018 17th Annual Mediterranean Ad Hoc Networking Workshop (MedHoc-Net), 2018, pp. 1-7.
- [17] D. Denkovski ; V. Atanasovski ; L. Gavrilovska ; J. Riihijärvi ; P. Mähönen, "Reliability of a radio environment Map: Case of spatial interpolation techniques", 2012 7th International ICST Conference on Cognitive Radio Oriented Wireless Networks and Communications (CROWNCOM), Stockholm, 2012, pp. 248-253.